A 7-Yr Climatological Study of Land Breezes over the Florida Spaceport

JONATHAN L. CASE, MARK M. WHEELER, AND JOHN MANOBIANCO

ENSCO, Inc., Cocoa Beach, and Applied Meteorology Unit, NASA, Kennedy Space Center, Florida

JOHNNY W. WEEMS AND WILLIAM P. ROEDER

45th Weather Squadron, U.S. Air Force, Patrick Air Force Base, Florida

(Manuscript received 11 May 2003, in final form 16 August 2004)

ABSTRACT

Seven years of wind and temperature data from a high-resolution network of 44 towers at the Kennedy Space Center and Cape Canaveral Air Force Station were used to develop an objective method for identifying land breezes, which are defined as seaward-moving wind shift lines in this study. The favored meteorological conditions for land breezes consisted of surface high pressure in the vicinity of the Florida peninsula, mainly clear skies, and light synoptic onshore flow and/or the occurrence of a sea breeze during the afternoon preceding a land breeze. The land breeze characteristics are examined for two events occurring under different weather regimes—one with light synoptic onshore flow and no daytime sea breeze, and another following a daytime sea breeze under a prevailing offshore flow. Land breezes were found to occur over east-central Florida in all months of the year and had varied onset times and circulation depths. Land breezes were most common in the spring and summer months and least common in the winter. The average onset times were ~4–5 h after sunset from May to July and ~6.5–8 h after sunset from October to January. Land breezes typically moved from the west or southwest during the spring and summer, from the northwest in the autumn, and nearly equally from all directions in the winter. Shallow land breezes (<150-m depth) were typically not associated with the afternoon sea breeze and behaved like density currents, exhibiting the largest temperature decreases and latest onset times. Deep land breezes (>150-m depth) were most often preceded by an afternoon sea breeze, had the smallest horizontal temperature gradients, and experienced a mean onset time that is 4 h earlier than that of shallow land breezes.

1. Introduction

a. Motivation

The onset of a land breeze at the Kennedy Space Center (KSC) and Cape Canaveral Air Force Station (CCAFS) is both operationally significant and challenging to forecast. The occurrence and timing of the nocturnal land breeze affect low-level winds, atmospheric stability, low temperatures, and fog development. Accurate predictions of the land breeze are especially critical for toxic material dispersion forecasts associated with space lift operations, because wind direction and low-level stability (both of which affect plume forecasts) can change noticeably with the passage of a land breeze front.

Several studies have analyzed the sea-breeze phenomena in great detail (Wakimoto and Atkins 1994; Atkins et al. 1995; Kingsmill 1995; Laird et al. 1995; Atkins and Wakimoto 1997; Wilson and Megenhardt 1997; Arritt 1993; Simpson 1996; Stephan et al. 1999); however, very few studies have examined the land breeze phenomena, particularly over relatively flat terrain, such as the Florida peninsula. The dearth in land breeze studies is not surprising because the phenomenon does not often lead to deep convection and, thus, does not have the safety and economic ramifications associated with sea breezes. Given the importance of the land breeze at KSC/CCAFS , the Applied Meteorology Unit was tasked by the U.S. Air Force 45th Weather Squadron to analyze the characteristics of land breezes over east-central Florida and to develop forecast tools based on these observed characteristics. The ultimate goal was to improve the reliability of daily land breeze occurrence forecasts across KSC/CCAFS, and to help to determine the timing, duration, speed, and direction of the land breeze.

b. Background

The traditional notion behind land breezes is that they are driven by nocturnal thermal contrasts caused

Corresponding author address: Jonathan L. Case, ENSCO, Inc., 1980 N. Atlantic Ave., Suite 230, Cocoa Beach, FL 32931.
E-mail: case.jonathan@ensco.com

by differential cooling between the land and water—the inverse of the sea breeze. Because the air in contact with the land cools faster than the air over the adjacent water body, a shallow mesoscale pressure gradient develops with higher surface pressure over the land than over the water. The resulting land breeze circulation has the appearance of a density current and is directed from the land to the sea near the surface, along with a corresponding return flow from sea to land above the land breeze. The land breeze circulation is generally much weaker than the sea breeze in both velocity and depth because the surface-based heat source for the land breeze (i.e., ocean) is much weaker than the heat source for the sea-breeze circulation (i.e., land; Atkinson 1981, 125–214), and higher static stability at night tends to diminish circulation intensity (Mak and Walsh 1976).

Another possible mechanism responsible for the nocturnal land breeze, particularly during the Florida summer months, is the modulation of the sea-breeze circulation by the Coriolis force and/or the prevailing synoptic flow. The Coriolis force rotates in a clockwise sense the onshore-directed wind field associated with the daytime sea-breeze circulation. After the land–water thermal contrast and corresponding mesoscale pressure gradient force weaken after dark, the wind field rotates from onshore to offshore because of the predominance of the Coriolis force (Yan and Anthes 1987). In addition, when the prevailing synoptic flow is directed offshore, a sharp sea-breeze front develops and moves inland, depending on the strength of the synoptic flow. As the land–sea thermal contrast weakens/reverses after dark, the sea breeze circulation opposing the synoptic flow also weakens. Consequently, the offshore synoptic flow overtakes the sea breeze and pushes the front back to the coast.

c. Previous studies on land breezes

Using observational data from the KSC Atmospheric Boundary Layer Experiment, (Taylor et al. 1990), Zhong and Takle (1992) examined the evolution of a sea and land breeze over east-central Florida from late May 1989. The authors suggested that the mesoscale pressure gradient was much less important in forcing the land breeze than the sea breeze. In their companion paper, Zhong and Takle (1993) used a boundary layer model to determine the sea- and land breeze evolution and balance of forces under various large-scale flow regimes. From these experiments, the authors found that an onshore wind greater than 5 m s^{-1} prevented the development of a land breeze. They also suggested that the strength of the land breeze was more sensitive to the prevailing large-scale flow and daytime surface heating in comparison with the magnitude of the nocturnal surface cooling over land. Their results suggest that the central Florida nocturnal land breeze during the summer months is primarily driven by the daytime sea breeze, large-scale flow, and the inertial oscillation.

Previous land breeze climatologies, both conducted in India, have been compiled by Sen Gupta and Chakravortty (1947) and Dekate (1968). In Sen Gupta and Chakravortty (1947), the authors constructed a 5-yr climatology of land breezes at Calcutta, consisting of monthly onset time frequencies, duration, wind direction, and temperature and humidity changes associated with the land breeze. Dekate (1968) compiled the monthly average frequency and onset times of both land and sea breezes in Bombay, with a primary emphasis on the sea breeze.

This paper presents the first multiyear observational study of land breezes over east-central Florida. Section 2 describes the data used to analyze individual events and develop a 7-yr land breeze climatology over KSC/CCAFS from February 1995 to January 2002. Section 3 presents two sample land breezes that exemplify the two prevalent classes of land breezes discussed in the 7-yr climatology. The results of the climatology are presented in section 5, and section 6 summarizes the paper.

2. Observational datasets

Four observational datasets were used to analyze land breezes and develop a multiyear climatology: the KSC/CCAFS mesonetwork, five 915-MHz Doppler radar wind profilers (DRWPs), mean sea level pressure (MSLP) reanalysis data, and archived surface observations from the Shuttle Landing Facility (TTS). These datasets, along with the procedures used for quality control, are described in the following subsections.

a. KSC/CCAFS towers

The dataset used to develop the climatology is the KSC/CCAFS mesonetwork, consisting of 44 observational towers (Fig. 1) with data archived every 5 min. The mesonet has an average station spacing of 5 km and measures temperature, dewpoint, and winds at various levels ranging from 1.8 to 150 m. The primary measurement levels for most towers are 1.8 (temperature and dewpoint), 3.7 (winds), and 16.5 m (winds and temperature). This study used the 1.8-m temperature and relative humidity (computed from temperature and dewpoint), 16.5-m wind and temperature, and the difference between the 1.8- and 16.5-m temperatures for near-surface stability.

All tower data were subject to quality control (QC) prior to analysis and processing for the land breeze climatology. The QC method included five routines, consisting of an unrealistic value check, a standard deviation check, a peak-to-average wind speed ratio check, a vertical consistency check, and a temporal consistency check (Lambert 2002).

b. 915-MHz Doppler radar wind profilers

Archived 915-MHz DRWP data from five profiler sites were used to supplement the subjective analysis of

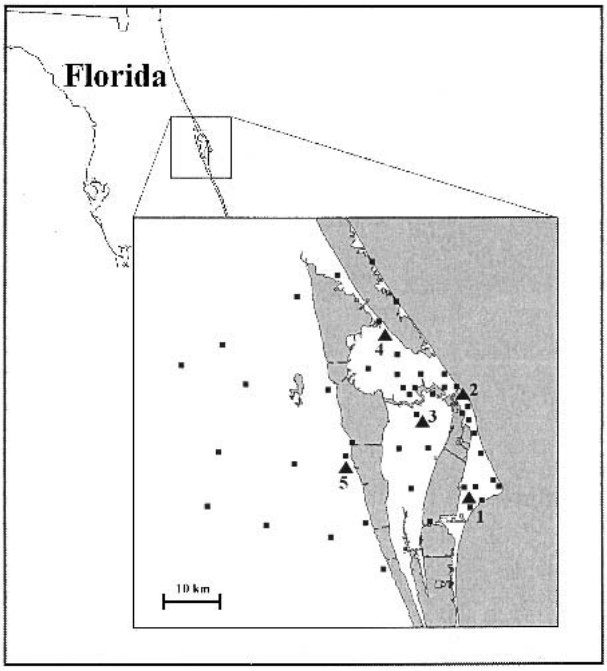

FIG. 1. The locations of the 44 KSC/CCAFS observational towers (squares) used to study land breezes and develop the 7-yr land breeze climatology over east-central Florida. The locations of the five 915-MHz DRWP sensors are given by triangles and labeled with numbers 1–5.

several individual land breeze events from November 1999 to August 2001. These data provide valuable boundary layer wind information from 130 to as high as 6000 m, depending on the meteorological conditions that affect the signal-to-noise ratio of the instrument. Under typical conditions, the 915-MHz profilers measure winds from 130 to approximately 3000 m. The gate-to-gate resolution of the instrument is about 100 m and measurements are available every 15 min.

The 915-MHz DRWP data were subjected to a set of automated QC algorithms (Lambert et al. 2003) based on the quality assessment routines described in Lambert and Taylor (1998), followed by a rigorous manual QC. The automated QC included checks of the length of the consensus averaging period, signal-to-noise ratio, unrealistic values, possible rain contamination, vertical shear magnitude, and spatial and temporal consistency. The quality-controlled data were used to examine the vertical structure of several land breeze events with depths greater than 150 m.

c. Mean sea level pressure reanalysis data

The National Centers for Environmental Prediction (NCEP) and National Center for Atmospheric Research (NCAR) have extensive reanalysis data dating back several decades (Kalnay et al. 1996). These data are available on a 2.5° latitude × 2.5° longitude grid and include many surface and upper-level meteorological variables (refer to http://www.cdc.noaa.gov/cdc/data.ncep.reanalysis.html). For this project, the NCEP–NCAR reanalysis MSLP grids were used in two ways. First, contoured images of MSLP fields were obtained over a subset region that covers the southeastern United States and surrounding waters of the Gulf of Mexico and Atlantic Ocean. These contoured images were subjectively examined to classify the large-scale flow associated with land breeze events. Second, the digital MSLP reanalysis data over this region were used to distinguish objectively between land breezes and wind shifts associated with pressure troughs or fronts (see section 4).

d. Shuttle landing facility hourly observations

As with the KSC/CCAFS towers and 915-MHz profilers, these hourly data were subject to QC, according to the methods discussed in Lambert (2001). The QC routine consists of an unrealistic value check, a standard deviation check, and a temporal consistency check. These observations were also used within the objective land breeze identification technique as described in section 4.

3. Two sample land breeze events

This section presents two land breeze events from 6 March and 12 May 2000. The 6 March event exemplifies a shallow, density current type of land breeze, where synoptic onshore flow shifted to offshore flow with the passage of the shallow land breeze front. The 12 May 2000 event illustrates a deep land breeze preceded by a daytime sea-breeze circulation, occurring under offshore-directed synoptic flow.

a. 6 March 2000 event

On the night of 6 March 2000, weak high pressure dominated the southeastern United States and the Florida peninsula (not shown). The prevailing surface wind flow was light ($\leq$2.5 m s^{-1}) and from the northeast (NE), and the skies were mostly clear with only patchy high clouds, creating ideal conditions for the development of a land breeze. A sharp land breeze boundary propagated eastward across KSC/CCAFS between 0500 and 0600 UTC. During the afternoon preceding the land breeze, the high temperature at Orlando, Florida (MCO), was 26°C, and no sea breeze was observed. The low temperature during the night of the land breeze was 12°C.

The land breeze reached the westernmost KSC/CCAFS towers just before 0500 UTC and moved east of these towers by 0515 UTC (Fig. 2a). The land breeze front progressed eastward during the next 45 min, reaching western Merritt Island by 0530 UTC (Fig. 2b), eastern Merritt Island by 0545 UTC (Fig. 2c), and the tip of Cape Canaveral by 0600 UTC (Fig. 2d). The land breeze moved across the entire KSC/CCAFS tower network in about 1.4 h.

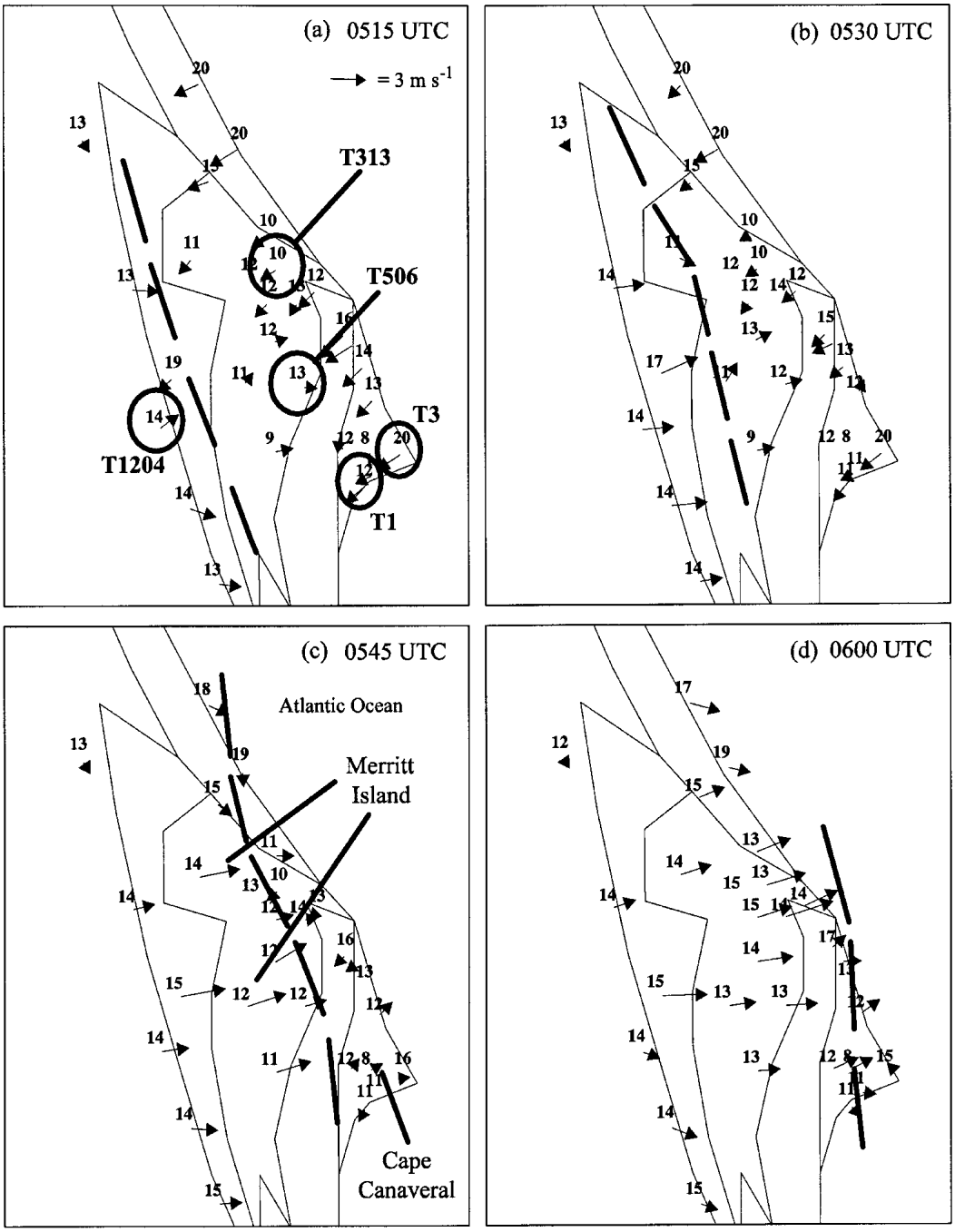

FIG. 2. KSC/CCAFS tower observations of 16.5-m winds and 1.8-m temperatures on 6 Mar 2000 at (a) 0515, (b) 0530, (c) 0545, and (d) 0600 UTC. The winds are given by arrows, with the tail centered on each station [speed scale provided in (a)], and 1.8-m temperatures (°C) are plotted above the wind arrows. The locations of towers 1, 3, 313, 506, and 1204 for subsequent figures are circled in (a) and major geographical features are given in (c). Thick dashed lines denote the location of the land breeze front.

The time series plots of wind direction at the KSC/CCAFS towers 1, 3, 506, and 1204 all show a distinct wind shift from onshore to offshore between 0500 and 0600 UTC (Fig. 3a). The post–land breeze wind direction was initially from the west (W), but gradually veered to the northwest (NW) during the remainder of the night. All time series indicate a decrease in 16.5-m temperatures associated with the land-breeze passage (Fig. 3b); however, the 1.8-m temperature changes were not as straightforward. Many of the 1.8-m temperatures

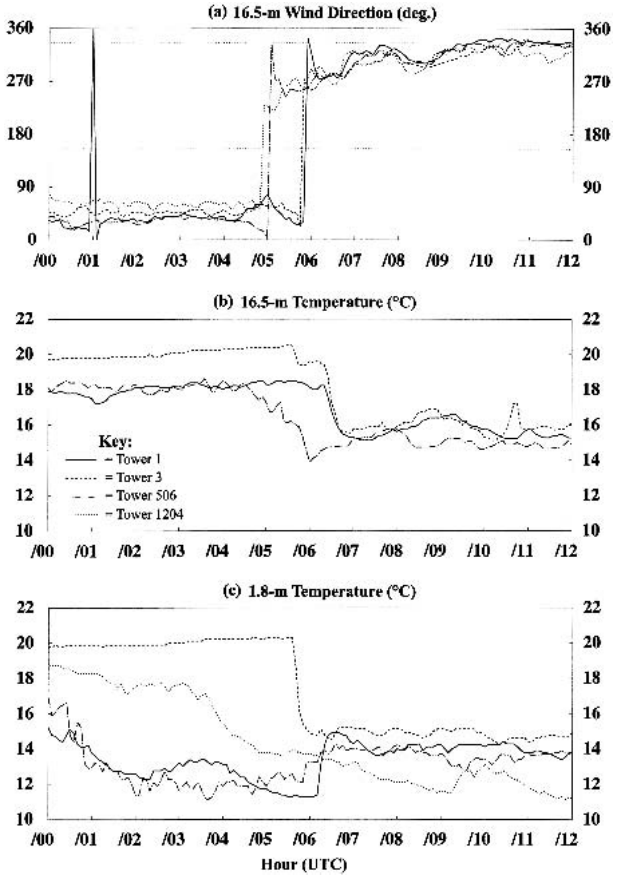

FIG. 3. Time series plots for KSC/CCAFS towers 1, 3, 506, and 1204, from 0000 to 1200 UTC 6 Mar 2000. The variables are (a) 16.5-m wind direction, (b) 16.5-m temperature (°C), and (c) 1.8-m temperature (°C). Note that 16.5-m temperatures are not available for tower 1204. The horizontal dotted lines in (a) differentiate between onshore and offshore wind direction. The key is provided in (b), and tower locations are shown in Fig. 2a.

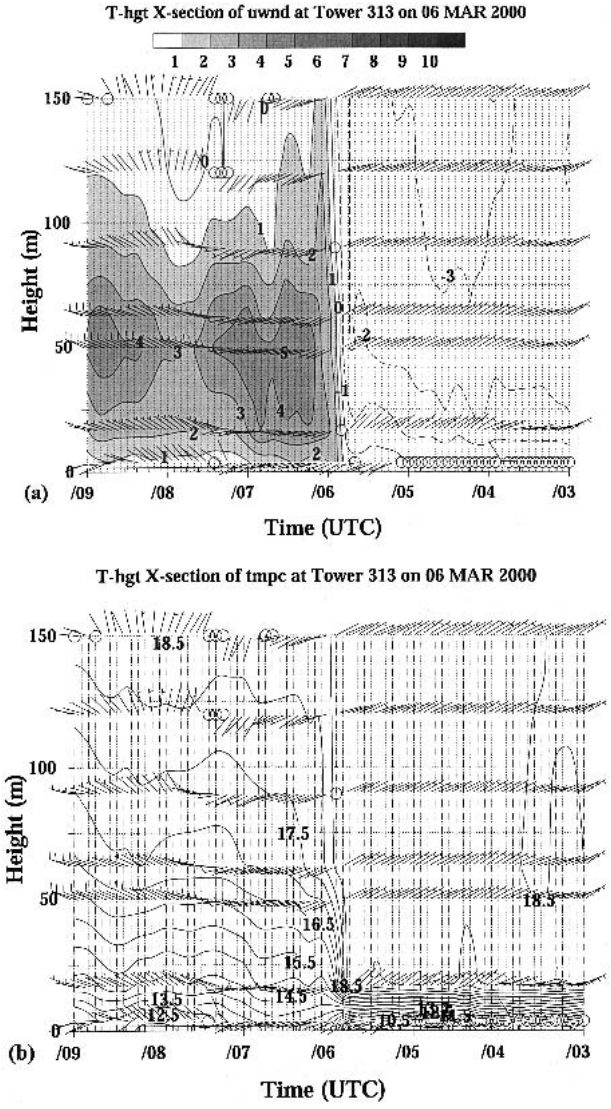

FIG. 4. Time–height cross sections at tower 313 from 0300 to 0900 UTC 6 Mar 2000 displaying wind vectors with (a) u wind components, and (b) temperatures. Time along the x axis increases from right to left and height along the y axis is given in meters. The u wind component in (a) is contoured in 1 m s^{-1} increments, with positive (westerly) u winds greater than 1 m s^{-1} shaded according to the scale provided. Temperature is contoured every 0.5°C in (b).

over Merritt Island increased by a few degrees following the passage of the land breeze, especially by 0600 UTC (see Fig. 2). The time series plots in Fig. 3c show 1.8-m temperature increases at towers 1 and 506 at about 0600 UTC.

It is interesting to note that although towers 1 and 3 are very close to each other (only ~5 km apart), they exhibited completely different 1.8-m temperature changes following the passage of the land breeze. The light NE wind flow maintained warm temperatures along the immediate coast at tower 3 prior to the land breeze. Once the land breeze front passed tower 3, the 1.8-m temperature dropped rapidly by about 5°C in 15 min (Fig. 3c). Conversely, at tower 1, there is enough fetch of land upstream under light NE flow to allow for radiational cooling and the development of a temperature inversion prior to the land breeze. This resulted in a 1.8-m temperature increase once the stronger winds of the land breeze eroded the shallow temperature inversion.

At the 150-m-tall tower 313 (location given in Fig. 2a), light NE flow of about 2.5 m s^{-1} prevailed at all levels until about 0600 UTC (Fig. 4a). Just prior to 0600 UTC, an abrupt wind shift occurred at all levels with the strongest W winds found at 50 m. Note that the W flow is much weaker and fleeting above 100 m, suggesting that the land breeze circulation is not much deeper than 100 m. This depth of the W flow is approximately an order of magnitude less than the observed depth of the easterly low-level flow that is associated with the sea-breeze circulation over east-central Florida and is similar to the depth observed by Ohara et al. (1989) in Tokyo, Japan.

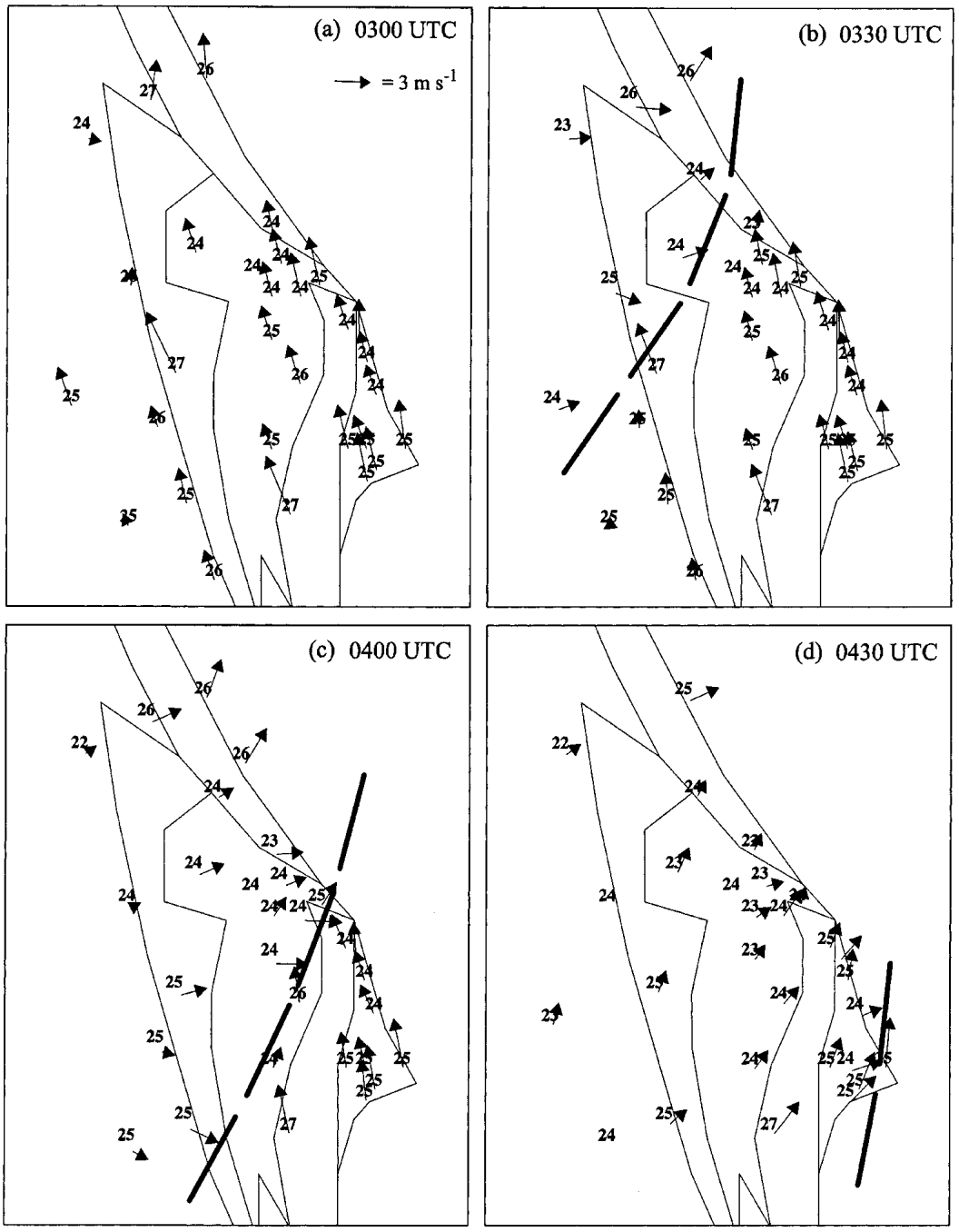

FIG. 5. KSC/CCAFS tower observations of 16.5-m winds and 1.8-m temperatures for 12 May 2000 at (a) 0300, (b) 0330, (c) 0400, and (d) 0430 UTC. The winds are given by arrows, with the tail centered on each station [speed scale provided in (a)], and 1.8-m temperatures (°C) are plotted above the wind arrows. Thick dashed lines denote the location of the land breeze front.

The thermal structure shown in Fig. 4b clearly depicts a dome of colder air following the passage of the land breeze, which behaved much like a shallow density current. Prior to the land breeze, the prevailing temperatures were about 18°C above a surface-based inversion layer. Following the land breeze passage, temperatures decreased by 2°−4°C in less then 30 min within the layer from 16.5 to 50 m. Near the surface, the strength of the temperature inversion decreased rapidly as the wind speeds increased and warmer air from aloft was transported to the surface through mechanical mixing.

b. 12 May 2000 event

Unlike the 6 March event, the 12 May land breeze followed a sea breeze from the previous afternoon. On the night of 12 May, a high pressure ridge was situated over the Bahamas extending across south Florida into the Gulf of Mexico (not shown), resulting in light southwesterly (SW) synoptic flow. The afternoon high temperature at MCO was 34°C, while the low temperature was 19°C during the night of the land breeze.

South (S) to southeast (SE) winds prevailed at 16.5 m prior to the land breeze passage (Fig. 5a). By 0330 UTC (Fig. 5b), the land breeze front had entered the KSC/CCAFS observational network extending from northern Merritt Island, southwestward to mainland Florida. The leading edge of the land breeze moved steadily to the E-SE over the next hour, reaching the tip of Cape Canaveral by 0430 UTC (Figs. 5c,d). Westerly winds of $\sim$3 m s^{-1} occurred behind the land breeze front. The postfrontal wind direction backed from W to the SW between 0330 and 0430 UTC, while the speeds decreased (Figs. 5b–d).

The cooling at 1.8 m associated with this land breeze was minimal with the passage of the front. At most stations, the temperatures remained nearly the same, but a few stations in the northern portion of KSC/CCAFS cooled by 1°C in 1 h. After the land breeze passage, the temperatures at most stations were generally above 22°C.

The time–height cross section at tower 313 depicts the land breeze passage just before 0400 UTC (Fig. 6a). A distinct wind shift from SE to SW is evident at all levels of tower 313. In fact, the wind shift is also apparent in the 915-MHz DRWP data up to about 1000 m (not shown). The post–land breeze winds were initially strongest between 0400 and 0500 UTC, and then weakened after 0500 UTC. The SW flow then strengthened at all levels after 0600 UTC, with a peak u wind component of 4 m s^{-1} at 125 m and 0730 UTC. Only a negligible temperature contrast occurred with the land breeze passage, except near the surface between 0500 and 0600 UTC, where a fleeting thermal inversion developed below 50 m because of calm surface winds (Fig. 6b).

Because this type of analysis of all of the land breezes over 7 yr would have been a very labor-intensive task, an objective method was designed to identify land breezes with minimal manual intervention. The remainder of this paper presents the methodology and results from a 7-yr climatology of land breezes across east-central Florida, focusing on the characteristics of the two types of land breezes presented in this section.

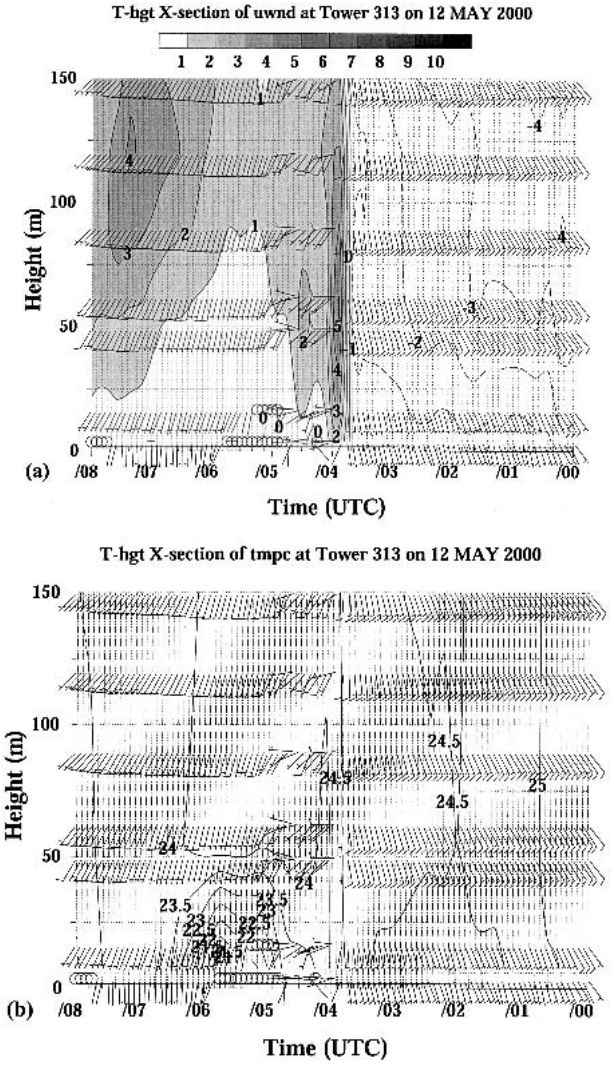

FIG. 6. Time–height cross sections at tower 313 from 0000 to 0800 UTC 12 May 2000 displaying wind vectors with (a) u wind components, and (b) temperatures. Time along the x axis increases from right to left and height along the y axis is given in meters. The u wind component in (a) is contoured in 1 m s^{-1} increments, with positive (westerly) u winds greater than 1 m s^{-1} shaded according to the scale provided. Temperature is contoured every 0.5°C in (b).

4. Methodology for developing a 7-yr climatology

An objective computer-based method was developed to identify land breeze events without including other wind shift lines, such as fronts or precipitation outflows. The time period between the hours of 0000 and 1300 UTC (1900−0800 LST) was examined for the presence of land breeze fronts during the period of record spanning from February 1995 to January 2002. The objective algorithm was designed to identify most land breeze events, while having a near-zero false-alarm rate.

The KSC/CCAFS tower data were analyzed to a grid with 1.25-km horizontal grid spacing using the two-pass Barnes (1973) objective analysis technique within the General Meteorological Package software, as described in Koch et al. (1983). The average mesonetwork station spacing and a Barnes convergence parameter of 0.9 yielded spectral responses greater than e^{-1} for wave-

TABLE 1. A list of the meteorological and data conditions that warrant a night to be removed from consideration for a land breeze in the objective land breeze identification program.

Condition	Reason(s) for rejection
Presence of a trough in archived MSLP data	Prevent the identification of a wind shift associated with a frontal or trough passage
Large MSLP changes (>5.0 hPa in 13 h) at TTS	Prevent the identification of a wind shift associated with a frontal or trough passage
Any report of precipitation or thunder at TTS between 0000 and 1300 UTC	(a) Avoid the identification of outflow boundaries; (b) occurrence of precipitation is highly unfavorable for land breeze development
More than 7 out of 14 hourly reports of cloud ceilings at TTS	Insufficient radiational cooling for land breeze development
More than 5 out of a possible 14 TTS cloud reports missing	Prevents the adequate determination of sufficiently clear skies (see condition above)
Mean nighttime, domain-wide 16.5-m wind greater than 3.5 m s^{-1}	Wind speeds too strong for development of land breeze (This criterion was established based on the daily subjective analysis from Oct 1999 to Apr 2000)
More than 4% of 5-min tower data missing between 0000 and 1300 UTC	Too much missing data, preventing adequate temporal continuity for tracking boundaries in the program

lengths longer than ~20 km. This objective analysis configuration helped to smooth out the small-scale features while retaining the land breeze signal of interest. Temperatures at 1.8 and 16.5 m, and u/v wind components at 16.5 m were analyzed to the grid every 5 min.

Prior to identifying and analyzing the movement of land breeze boundaries, several rules were applied to remove from consideration any nights that experienced meteorological conditions that were unfavorable for land breeze development, or that had too much missing data (see Table 1). The algorithm identified boundaries from the analysis grids based on a distinct shift between near-coastal onshore and inland offshore wind directions, and tracked the boundary features across the grid. Based on the orientation of east-central Florida coastline (see Fig. 1), offshore winds were given by wind directions between 180° and 335°, while all other wind directions were considered onshore. Boundaries were determined by wind-direction changes of at least 20° across a 5-km distance (i.e., four analysis grid spacings). The 20° criterion was empirically determined to maximize the number of identified events while retaining a near-zero false-alarm rate.

To ensure temporal continuity, the presence of the boundary was required at every 5-min analysis time between start and stop times. The start time is considered the time at which the boundary was first identified in the domain. The stop time represents the time of complete passage of the land breeze front. The land breeze boundary start and stop times were determined based on time and space continuity of seaward-moving wind shift lines. Offshore winds associated with the land breeze often continued for several hours after the stop time of the frontal passage.

The algorithm successfully identified 393 land breeze events during the 7-yr period, which were all validated by subjectively examining the wind and temperature fields during 0000−1300 UTC for meteorological consistency and realism. Some events may have been missed in the climatology such as land breezes that transpired during generally overcast nights, or wind shifts that occurred when the prevailing winds were already slightly offshore (e.g., ~190°) prior to the land breeze front.

Out of the 393 land breezes, 264 events that affected the 150-m-tall tower 313 were examined and classified into deep versus shallow events. (Many land breezes could not be analyzed at tower 313 because of missing data at various levels.) Deep events were considered those in which the offshore wind component occurred at all observation levels of tower 313 up through 150 m. The shallow events had an offshore flow depth less than 150 m and often had a gradual slope at the leading edge of the front.

The land breezes were further divided into minimal convective (MC; October–May) and peak convective months (PC; June–September), and categorized by weather regime to determine land breeze characteristics under various weather scenarios. The occurrence or absence of a sea breeze (SB or no SB, respectively) during the day preceding each land breeze event was also noted. Sea-breeze occurrence/absence was determined by examining tower data between 1200 and 0000 UTC for a distinct onshore wind shift, or increase in onshore wind speed under synoptic onshore flow.

The direction from which the land breeze moved was determined by computing the resultant direction from the average u and v wind components for 1 h after the land breeze frontal passage at all towers that experienced the passage. Similarly, the pre–land breeze mean wind was determined for the hour prior to land breeze passage at all towers that experienced the passage.

Last, to determine the impact of land breezes on temperature and low-level stability, composite changes were generated by averaging each quantity at tower locations that experienced a land breeze passage. The values were averaged every 5 min at ±60 min of the land breeze passage. The composite quantities normalized to the time of the land breeze passage isolated the impact of the land breeze on temperature and stability.

TABLE 2. A summary of the number of land breezes identified by the objective algorithm for each month from Feb 1995 to Jan 2002. The months and year with a minimum number of land breezes are given by boldface type, whereas the months and year with the maximum number of events are shown in italic font.

Year	Jan	Feb	Mar	Apr	May	Jun	Jul	Aug	Sep	Oct	Nov	Dec	Annual
1995		1	2	8	8	4	8	4	9	3	6	2	55
1996	4	6	2	9	4	8	5	5	6	5	2	4	60
1997	3	3	5	3	6	3	6	5	6	3	1	0	**44**
1998	1	3	2	5	12	6	7	3	**0**	3	5	2	49
1999	5	8	12	*13*	6	2	*13*	7	2	3	3	2	*76*
2000	2	2	8	6	6	2	5	9	2	6	5	3	56
2001	2	6	4	6	5	3	4	10	1	**0**	6	2	49
2002	4												(4)
Tot	21	29	35	50	47	28	48	43	26	23	28	15	393
Avg	3.0	4.1	5.0	7.1	6.7	4.0	6.9	6.1	3.7	3.3	4.0	2.1	56.1

5. The 7-yr composite results

a. Land breeze occurrence by month

This section provides a summary of the 7-yr composite climatology of land breeze events at the KSC/CCAFS towers from February 1995 to January 2002. The number of monthly land breezes ranged from 0 to 13 in any one month (Table 2), with the mean number of events peaking in April and May at about 7 and a secondary maximum of 6−7 in July and August. The minimum mean of two events per month occurred in December. The smaller number of land breezes during June and September as compared with the rest of summer was probably due to extensive precipitation and cloud cover during these months, which experienced the highest mean monthly rainfall for the period of record (Table 3).

The probable reasons for the peak in April are the prevalence of a surface high pressure ridge, the decreased influence of synoptic-scale frontal systems, the increased occurrence of daytime sea breezes, and the relatively large diurnal temperature variation. The maximum number of land breezes during July and August can be attributed to the prevalence of weak surface pressure gradients and nearly daily sea breezes. The smaller number of land breezes during December and January results from the prevalence of synoptic-scale systems, which preclude the development of a land breeze.

b. Land breeze onset times

1) MONTHLY DISTRIBUTION

From September to January, the mean onset time was between 6.5 and 8 h after sunset, whereas the average onset time was generally between 4 and 5 h after sunset from February to August (Fig. 7). With the exception of the February anomaly, these results indicate an annual trend that is inversely proportional to the frequency of sea breezes across central Florida. Earlier (later) onset times during the spring and summer (autumn and winter) months correspond with higher (lower) sea-breeze occurrences. It is important to note, however, that large variations occurred about the mean, so the annual trend in the mean onset times may not be statistically significant.

2) TOWER 313 RESULTS

A distinct difference in the timing of deep versus shallow land breezes at tower 313 can be seen in Fig. 8a. The deep land breeze events peak sharply between 3 and 7 h after sunset, with few occurrences after 9 h. Meanwhile, the shallow land breezes have a broader maximum between 7 and 12 h after sunset and no occurrences before 4 h.

Deep land breezes were typically preceded by a sea breeze during the previous afternoon (Fig. 8b). Deep circulations were much less common when not preceded by a sea breeze. The SB deep circulations appear to be normally distributed about a mean of ~4−5 h. Meanwhile, the no SB deep circulations do not appear to be normally distributed, and tended to occur after 3 h; however, the sample size of the no SB deep events was quite small. Contrary to the deep circulations, the shallow land breezes were typically not associated with preceding sea breezes because few differences occur in the distributions of onset time between SB and no SB events (Fig. 8c).

By examining the land breezes that followed an afternoon SB, the deep land breezes tended to begin between 10 and 14 h after the SB onset time (Fig. 8d). Meanwhile, the majority of shallow land breezes following a SB occurred between 16 and 20 h after the SB

TABLE 3. Monthly mean rainfall (cm) at the Shuttle Landing Facility for the period of record from Feb 1995 to Jan 2002.

	Jan	Feb	Mar	Apr	May	Jun	Jul	Aug	Sep	Oct	Nov	Dec
Mean rainfall	8.3	5.3	12.0	4.8	5.6	18.8	14.4	15.1	21.5	12.5	6.4	6.6

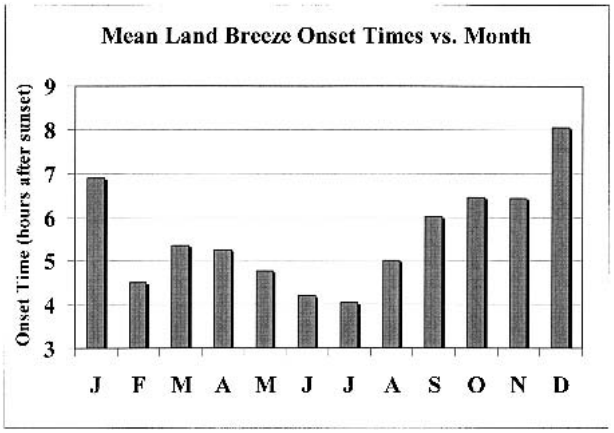

FIG. 7. The mean land breeze onset time as a function of month, given in hours after sunset.

onset time, and these events were probably not associated with the daytime SB. This large time separation was typically caused by an early SB onset time, followed by a late land breeze onset time during onshore (easterly) synoptic flow.

c. *Land breeze directions*

1) MONTHLY DISTRIBUTION

During October and November, more than 2 times as many land breezes came from the NW as compared with other directions, whereas land breezes from the SW and W were most prevalent in the spring and summer (Fig. 9a). Land breezes during the winter months were uniformly distributed among SW, W, and NW, slightly favoring the NW direction. The NW land breezes experienced a maximum in October and November (16) and a secondary maximum in March (13). Meanwhile, the frequency of SW and W land breezes increased gradually from December to March (~5–10) and then more sharply from March to April (~10–20, Fig. 9a).

The pre–land breeze wind directions do not show such clear tendencies; however, some discernable relationships do exist. The distribution of pre–land breeze winds from the north (N) as a function of month closely follows the frequencies of the NW land breeze directions (Fig. 9b). North winds were 2–3 times more likely than other directions prior to the land breeze during October and November. Meanwhile, S and SE winds

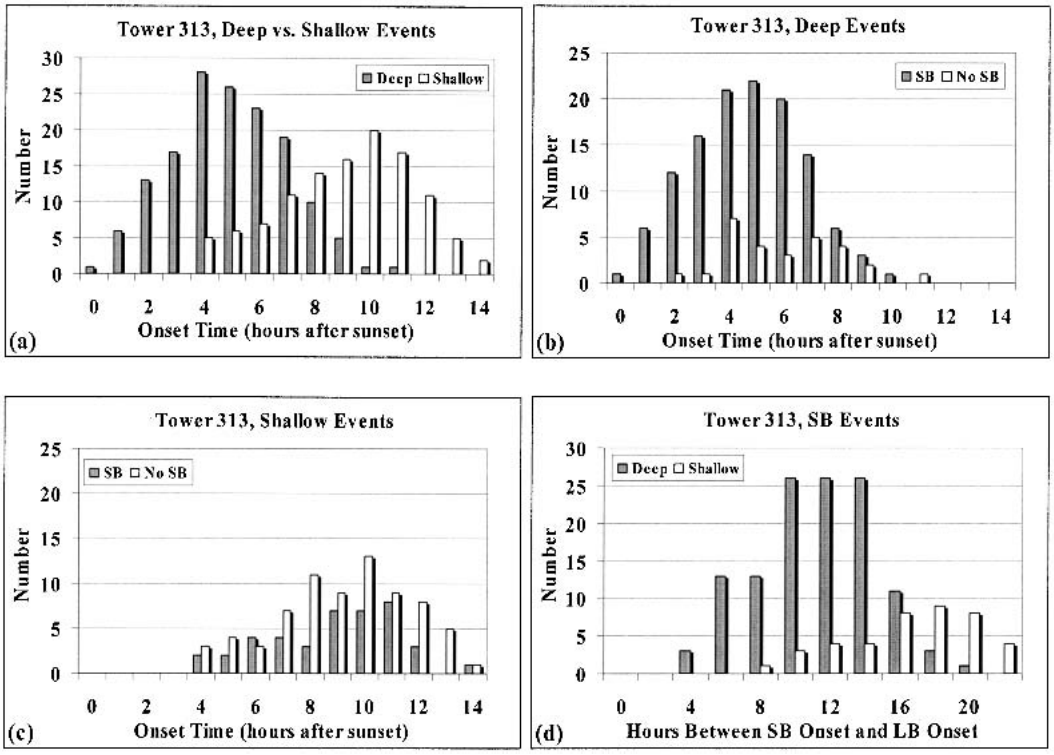

FIG. 8. The distributions of land breeze onset times (in hours after sunset) at tower 313 for all months from Feb 1995 to Jan 2002. The distributions are shown for (a) deep (>150-m depth) vs shallow (<150-m depth) circulations, (b) SB/no SB during the afternoon preceding the land breeze for all deep circulations, and (c) SB/no SB during the afternoon preceding the land breeze for shallow circulations. (d) The distribution of elapsed times between the SB and LB onset times are shown for deep vs shallow events for all land breezes that had a sea breeze during the preceding afternoon.

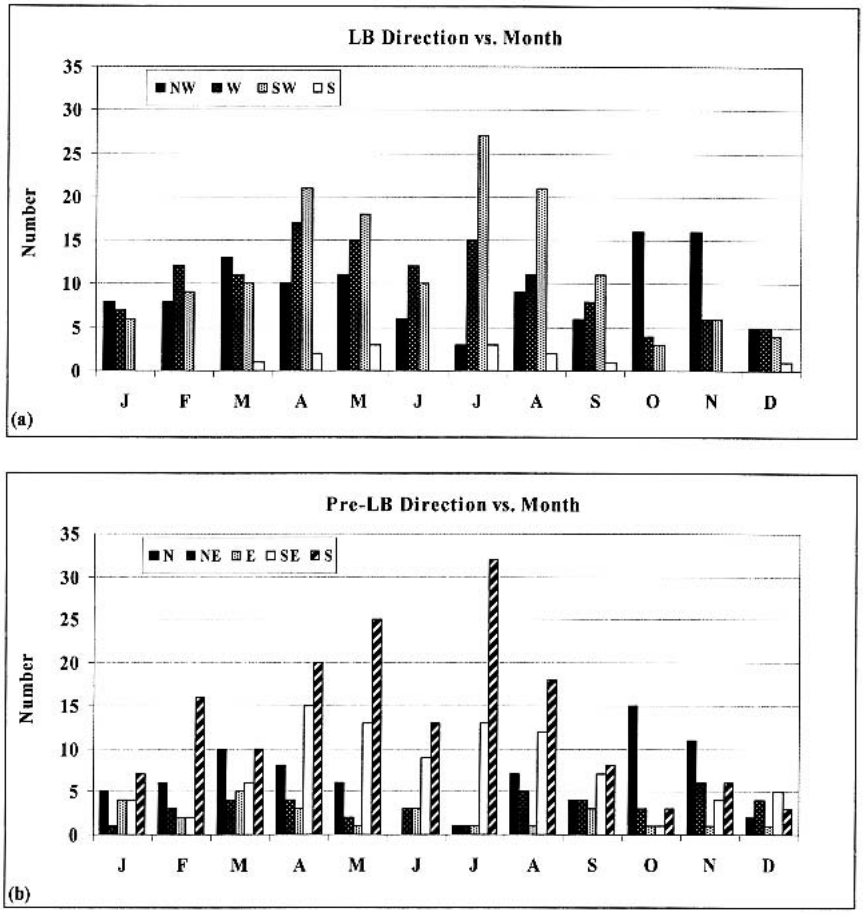

FIG. 9. The distributions of the post–land breeze and pre–land breeze wind direction as a function of month. (a) The monthly distributions of post–land breeze directions for all events, and (b) the monthly distributions of pre–land breeze directions for all events from Feb 1995 to Jan 2002. The land breeze direction is given by the mean wind for 1 h following the land breeze frontal passage at all towers that experienced a land breeze frontal passage.

prior to a land breeze were generally 2–4 times more common than other directions from April to August. In general, east (E) and northeast (NE) winds were relatively uncommon prior to a land breeze frontal passage.

2) TOWER 313 RESULTS

According to Fig. 10a, nearly all land breezes at tower 313 that came from the NW were shallow events, especially during the MC months. Meanwhile, about 2 times as many deep land breezes came from the SW in comparison with shallow land breezes in both the MC and PC months. For the pre–land breeze wind direction, the greatest disparity is found in the N and S categories. When N winds preceded a land breeze during the MC months, most events tended to be shallow, but when S winds preceded a land breeze at any time of the year, most land breezes had a deep circulation (Fig. 10b). This distribution indicates that the most common wind regimes associated with land breezes were S winds shifting to SW or W, and N winds backing to NW.

The SW and W land breeze directions for SB days were the most common categories for deep circulations (Fig. 10c). The next most frequent directions of deep land breezes were W and SW for no SB days. The NW land breezes rarely had deep circulations. The most prevalent pre–land breeze wind directions for deep circulations were S and SE winds for SB days (Fig. 10d). The S and SE pre–land breeze wind directions for SB days made up 87% of the deep/SB events, and 71% of all deep events (SB and no SB).

For shallow land breeze circulations, the pre– and post–land breeze wind directions are more evenly distributed in comparison with deep land breezes, but still favor particular regimes. The most prevalent shallow land breezes came from the NW during the MC months and were not associated with a SB, followed by W and SW directions, which are also not associated with a SB (no SB: October−May in Fig. 10e). For shallow land

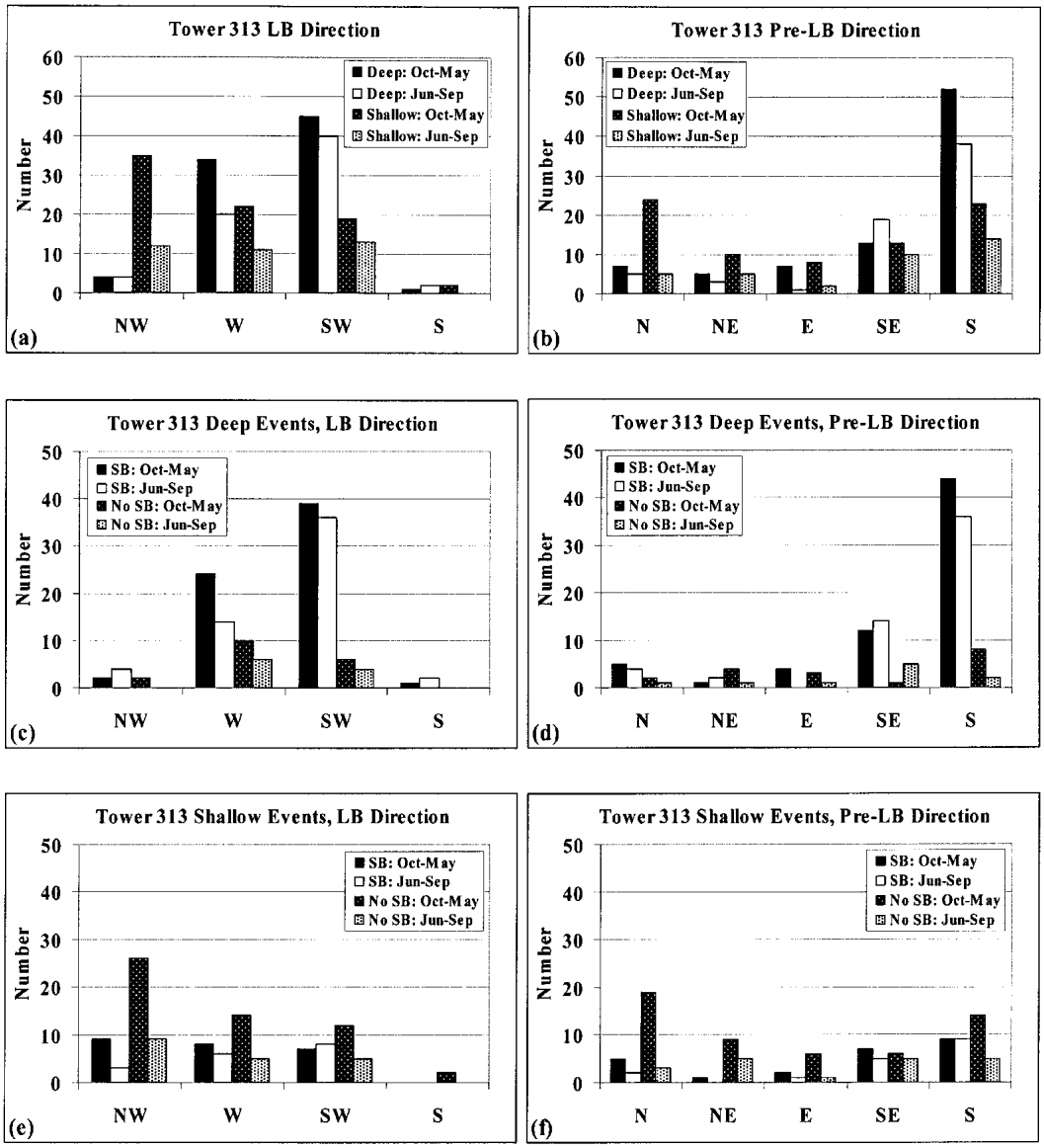

FIG. 10. The distribution of post–land breeze (LB) and pre–LB wind directions at tower 313 during the MC months (Oct–May) and PC months (Jun–Sep) for the following combinations: (a) LB direction for deep vs shallow events, (b) pre–LB direction for deep vs shallow events, (c) LB direction of deep events for the occurrence (SB) vs absence of a sea breeze (no SB) during the preceding afternoon, (d) pre–LB direction of deep events for SB vs no SB, (e) LB direction of shallow events for SB vs no SB, and (f) pre–LB direction of shallow events for SB vs no SB. Note that the *y* axis ranges from 0 to 60 in (a) and (b), and from 0 to 50 in (c)–(f).

breezes during SB days, the occurrence is evenly distributed among the NW, W, and SW directions. The pre–land breeze wind direction for shallow events are distributed across all categories. The most common directions preceding the land breeze front were N and S for no SB cases during the MC months (Fig. 10f).

3) RELATION TO LARGE-SCALE FLOW

By decomposing the land breezes into SB and no SB events, the relationship between the surface synoptic flow direction and the land breeze direction yields quite disparate distributions during the MC months (Figs. 11a and 11c). When a land breeze followed a sea breeze, the synoptic flow was primarily offshore and the land breeze typically came from the SW or W (Fig. 11a). When a sea breeze did not precede a land breeze, the synoptic flow was almost always from an onshore direction (Fig. 11c).

During the PC months, most land breezes were preceded by a daytime sea breeze, came from a SW or W direction, and occurred under SW or W synoptic flow

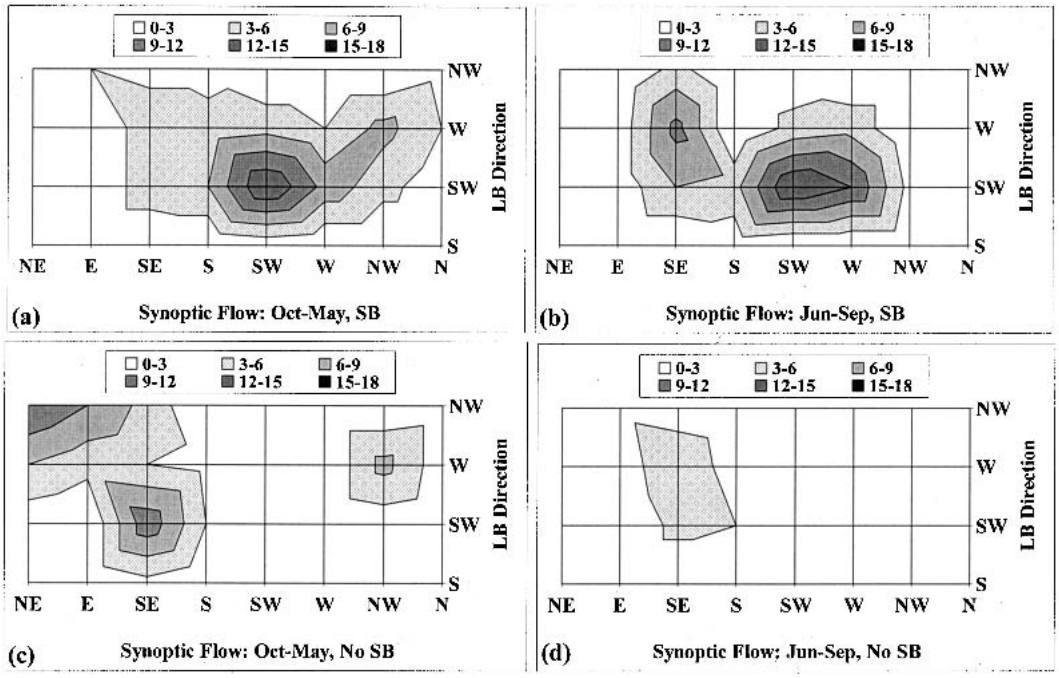

FIG. 11. The frequency distributions of land breeze directions as a function of the synoptic flow direction (mean sea level pressure), based on a categorization of events into MC (Oct–May) vs PC months (Jun–Sep) and events with and without an antecedent SB. Events preceded by a sea breeze are shown in (a) Oct–May, and (b) Jun–Sep. Events without a preceding sea breeze are shown in (c) Oct–May, and (d) Jun–Sep.

(Figs. 11b and 11d). A secondary maximum of W and SW land breezes occurred under SE synoptic flow with an antecedent sea breeze (Fig. 11b). Land breeze events that were not preceded by a sea breeze were quite uncommon during the PC months (Fig. 11d), because sea breezes occur on almost a daily basis in Florida.

Both land breeze events shown in section 3 fell into the most favored relationships of Fig. 11. The 6 March 2000 shallow event had a W-NW land breeze direction under synoptic flow from the NE, with no daytime sea breeze (Fig. 11c). The 12 May 2000 deep event experienced a land breeze direction from the SW under prevailing SW synoptic flow with the occurrence of a daytime sea breeze (Fig. 11b).

d. Composite changes in temperature and near-surface stability

1) MINIMAL CONVECTIVE MONTHS (OCTOBER–MAY)

At 1.8 m, land breezes during the MC months tended to have a warming effect, particularly for events with W winds behind the boundary (Fig. 12a). For the hour prior to the land breeze (−60 to 0 min), the mean temperature change rate at 1.8 m was about $-0.5°C\ h^{-1}$. After the boundary passage, the W land breezes experienced a warming rate of about $0.3°C\ h^{-1}$ for approximately 30 min. The NW land breezes had a slightly smaller impact on 1.8-m temperatures because their passage only slowed the rate of cooling for the first 30 min, with a slight warming rate thereafter. The SW land breeze had the smallest impact on the mean change rate of the 1.8-m temperatures.

At 16.5 m, land breeze passages during the MC months typically behaved as density currents as indicated by a net cooling (Fig. 12b). In fact, the mean 16.5-m temperature change for each land breeze regime was nearly opposite to the 1.8-m temperature change. The W (SW) land breeze had the greatest (least) warming influence at 1.8 m, whereas the W (SW) land breeze had the greatest (least) cooling impact at 16.5 m. At both heights, the NW land breeze aligned most closely with the overall mean temperature change rates (ALL in Fig. 12b).

The difference between the 16.5- and 1.8-m temperatures, approximating the near-surface stability, also showed variations between the different land breeze directions. The near-surface layer was almost always stable prior to land breeze passages ($T_{16.5} > T_{1.8}$), due to light winds favoring the development of both a radiation inversion and land breeze. The land breeze passages, however, acted to decrease the 1.8- to 16.5-m stability, probably because of mechanical mixing at the leading edge of the land breeze front. As seen in Fig. 12c, the near-surface layer was the least stable during nights with SW land breezes, and the SW land breeze passage also had the least impact on the rate of stability

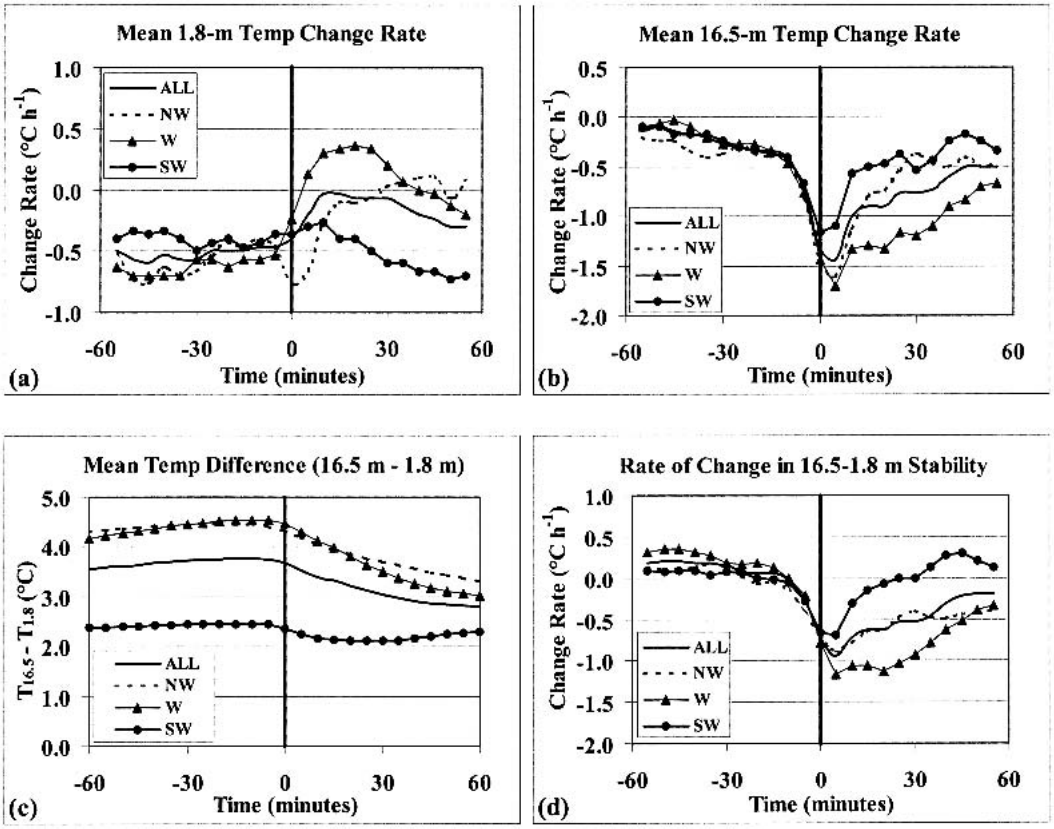

FIG. 12. Mean temperatures at ±60 min relative to land breeze passages during the MC months (Oct–May) for all land breezes (ALL), and for events with post–land breeze winds from the NW, W, and SW; (a) 1.8-m temperature change rate (°C h^{-1}), (b) 16.5-m temperature change rate (°C h^{-1}), (c) mean difference between the 16.5- and 1.8-m temperatures (layer stability; $T_{16.5} - T_{1.8}$; °C), and (d) rate of change in the difference between the 16.5- and 1.8-m temperatures (rate of change in stability; °C h^{-1}). Temperature and stability change rates were computed every 5 min using centered differences. The thick vertical line at 0 min in each panel represents the time of the land breeze passage.

decrease (Fig. 12d). The W and NW land breezes had comparable low-level stability values (Fig. 12c); however, the W land breeze experienced the largest and most sustained rate of decrease in the stability (Fig. 12d). These results suggest that the W land breezes had the strongest impact on temperatures and stability, and that the SW land breezes had the least influence on temperatures and stability across KSC/CCAFS.

2) PEAK CONVECTIVE MONTHS (JUNE–SEPTEMBER)

Temperature and stability data for the PC months show similarities as well as some differences from the MC land breeze events. As in the MC months, the 1.8-m temperatures experienced about a -0.5°C h^{-1} temperature change rate prior to the land breeze passage; however, for the hour following the land breeze onset, the temperature change rate increased only gradually (Fig. 13a), unlike the rather abrupt change in the rate shortly after the land breeze passage during the MC months (Fig. 12a). The exception is the SW land breezes, which did not experience much change in the temperature change rate for both MC and PC months.

The 16.5-m temperature change rate during the PC months was much different than MC months, except for NW land breezes. The 16.5-m temperature change rate for W and SW land breezes remained nearly constant following the land breeze passage, whereas the NW land breeze had a brief increase in cooling (Fig. 13b). A comparison between the 16.5-m temperature change rates of the MC (Fig. 12b) and PC land breezes suggests that land breezes during the cooler, drier MC months tended to be driven more by density current dynamics (i.e., land−sea thermal contrasts), whereas the land breezes during the PC months did not exhibit density current characteristics (except for possibly the NW land breeze).

As expected, the low-level stability between 1.8 and 16.5 m was, on average, lower during the PC months (Fig. 13c). Similar to the MC results (Fig. 12c), the stability was lowest for SW land breezes. Only the NW

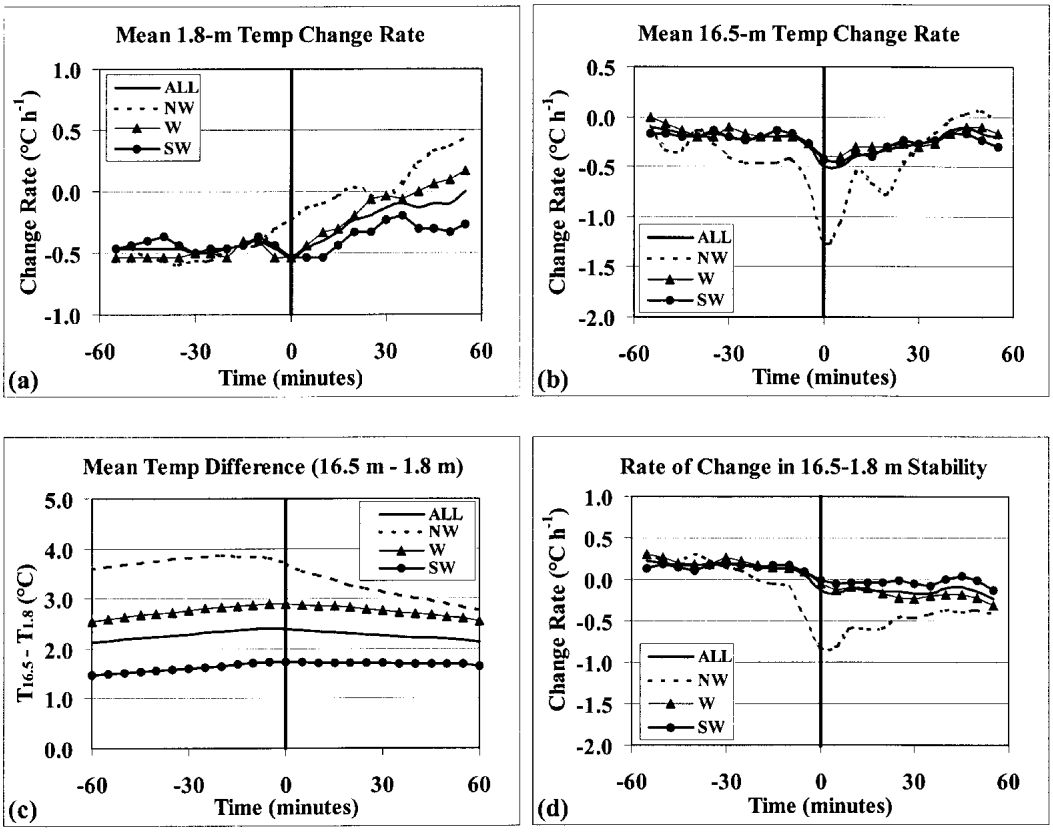

FIG. 13. As in Fig. 12, but during the PC months (Jun–Sep).

land breeze during the PC months resulted in any substantial decrease in the mean stability of this layer following the land breeze passage. In Fig. 13d, the stability change rate in the NW land breezes shows a decrease nearing $-1.0°C\ h^{-1}$ at the onset time, followed by a gradual increase. As compared with the MC months where the near-surface stability decreased abruptly at the time of land breeze passage, the near-surface stability changes associated with land breezes during the PC months were generally much smaller.

3) SEA-BREEZE VERSUS NO-SEA-BREEZE EVENTS (ALL MONTHS)

At 1.8 m, the SB type experienced a mean cooling rate of $-0.5°C\ h^{-1}$ for the hour preceding the land breeze passage, with a slight warming impact during the hour following passage ($\sim -0.3°C\ h^{-1}$ temperature change rate, Fig. 14a). Meanwhile, the no-SB type had a cooling rate of $-1.0°C\ h^{-1}$ before passage, warming to slightly above $0°C\ h^{-1}$ in the hour following the land breeze passage (Fig. 14a). At 16.5 m, the contrast between the two land breeze types is much more prevalent. Only a small cooling effect ($\sim -1.0°C\ h^{-1}$ for less than 10 min) is found with the SB type events; however, the no SB events experience much more cooling, with temperature change rates less than $-2.0°C\ h^{-1}$ associated with the land breeze passage, and only a gradual increase to $-1.0°C\ h^{-1}$ in the hour following the frontal passage. The temperature composites of Fig. 14 support the notion that cool-season land breezes typically behave like shallow density currents whereas other mechanisms appear to be responsible for the deep land breezes observed during the warm-season months.

6. Summary

This paper presented the first multiyear observational study of land breezes over east-central Florida. This analysis was enabled by the high-resolution tower network over KSC/CCAFS, which allowed for continuous tracking of convergent boundaries along the leading edge of land breezes.

Using the tower winds at 16.5 m interpolated to a high-resolution analysis grid every 5 min, an objective algorithm was developed to track these boundaries in both space and time. This algorithm was designed to identify wind shift lines propagating toward the coast, separating near-coast onshore from inland offshore winds.

During the 7-yr period of record, there were 393 total

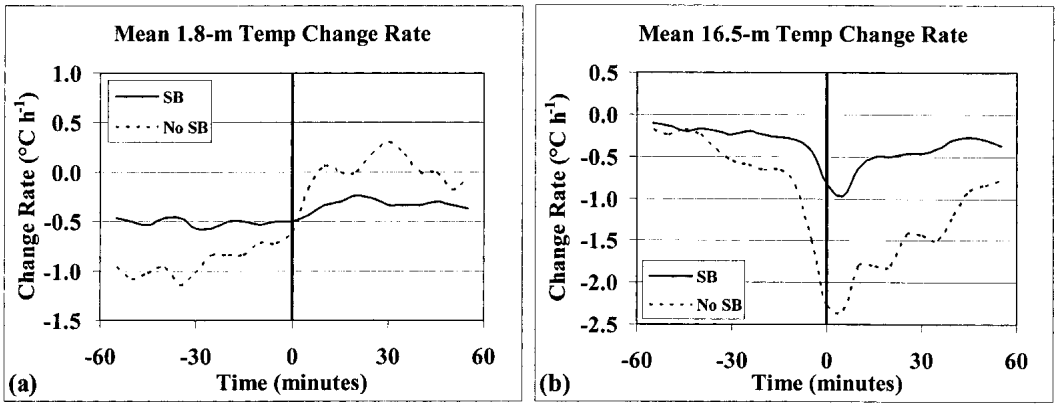

FIG. 14. Mean temperatures at ±60 min relative to land breeze passages for SB (solid line) and no-SB events (dashed line): (a) 1.8-m temperature change rate (°C h^{-1}), (b) 16.5-m temperature change rate (°C h^{-1}). Temperature change rates were computed every 5 min using centered differences. The thick vertical line at 0 min in each panel represents the time of the land breeze passage.

land breeze events identified and validated, 248 during the months from October to May, and 145 during the months from June to September. Land breezes were most common during the midspring and midsummer months (April and May, and July and August, respectively), and least common in December and January. The average onset times were ~4–5 h after sunset from May to July and ~6.5–8 h after sunset from October to January.

There were 264 events examined at tower 313 over Merritt Island, Florida, which were used to compare the characteristics of deep (depth > 150 m) versus shallow land breezes (depth < 150 m). Regardless of the time of year, land breezes with deep circulations had an onset time about 4 h earlier than shallow circulations. Over 80% of deep events had sea breezes the preceding afternoon, whereas less than 40% of shallow land breezes had sea breezes preceding them. These results suggest that the early, deep-circulation land breezes may be related to the daytime sea-breeze circulations. The shallow land breezes were probably density currents not associated with the afternoon sea breeze, and formed by radiational cooling over the interior of the Florida peninsula. Deep land breezes typically came from the W or SW year-round while shallow land breezes favored the NW direction during the cooler months.

The composite changes in 16.5-m temperatures at ±60 min of the land breeze passages indicated that the land breeze often behaved like a density current during the cooler months (October–May), particularly for events that were not preceded by a sea breeze during the afternoon hours. During June to September, only the NW land breeze showed signs of a density current, whereas all other land breeze directions had virtually no cooling associated with the frontal passage.

The combination of earlier land breeze onset times during the summer, a high frequency of sea-breeze occurrence, markedly deeper circulations, and minimal temperature contrast suggest that physical mechanisms other than differential cooling are responsible for the summer land breezes. The results from this paper suggest that the summer land breezes may develop from interactions between the synoptic flow and the daytime sea-breeze circulation. Future efforts could include modeling both idealized scenarios and actual events of deep land breezes that follow daytime sea-breeze circulations, in order to understand the physical processes behind such land breezes.

Acknowledgments. The authors thank Ms. Winifred Lambert, Dr. David Short, and Dr. Frank Merceret for their constructive suggestions during the task and their thorough reviews of the manuscript. The authors also appreciate the constructive comments from three anonymous reviewers who helped to improve the quality and focus of the paper.

Mention of a copyrighted, trademarked, or proprietary product, service, or document does not constitute endorsement thereof by the authors, ENSCO, Inc., the Applied Meteorology Unit, the National Aeronautics and Space Administration, or the U.S. Government. Any such mention is solely for fully informing the reader of the resources used to conduct the work reported herein.

REFERENCES

Arritt, R. W., 1993: Effects of the large-scale flow on characteristic features of the sea breeze. *J. Appl. Meteor.,* **32,** 116–125.

Atkins, N. T., and R. M. Wakimoto, 1997: Influence of the synoptic-scale flow on sea breezes observed during CaPE. *Mon. Wea. Rev.,* **125,** 2112–2130.

——, ——, and T. M. Weckwerth, 1995: Observations of the sea-breeze front during CaPE. Part II: Dual-Doppler and aircraft analysis. *Mon. Wea. Rev.,* **123,** 944–969.

Atkinson, B. W., 1981: *Meso-scale Atmospheric Circulations*. Academic Press, 495 pp.

Barnes, S. L., 1973: Mesoscale objective analysis using weighted time-series observations. NOAA National Severe Storms Laboratory Tech. Memo. ERL NSSL-62, 60 pp.

Dekate, M. V., 1968: Climatological study of sea and land breezes over Bombay. *Indian J. Meteor. Geophys.,* **19,** 421–442.

Kalnay, E., and Coauthors, 1996: The NCEP/NCAR 40-Year Reanalysis Project. *Bull. Amer. Meteor. Soc.,* **77,** 437–471.

Kingsmill, D. E., 1995: Convection initiation associated with a sea-breeze front, a gust front, and their collision. *Mon. Wea. Rev.,* **123,** 2913–2933.

Koch, S. E., M. DesJardins, and P. J. Kocin, 1983: An interactive Barnes objective map analysis scheme for use with satellite and conventional data. *J. Appl. Meteor.,* **22,** 1487–1503.

Laird, N. F., D. A. R. Kristovich, R. M. Rauber, H. T. Ochs III, and L. J. Miller, 1995: The Cape Canaveral sea and river breezes: Kinematic structure and convective initiation. *Mon. Wea. Rev.,* **123,** 2942–2956.

Lambert, W. C., 2001: Statistical short-range forecast guidance for cloud ceilings over the Shuttle Landing Facility. NASA Kennedy Space Center Contractor Rep. CR-2001-210264, 45 pp. [Available from ENSCO, Inc., 1980 N. Atlantic Ave., Suite 230, Cocoa Beach, FL 32931.]

——, 2002: Statistical short-range guidance for peak wind speed forecasts on Kennedy Space Center/Cape Canaveral Air Force Station: Phase I results. NASA Kennedy Space Center Contractor Rep. CR-2002-211180, 39 pp. [Available from ENSCO, Inc., 1980 N. Atlantic Ave., Suite 230, Cocoa Beach, FL 32931.]

——, and G. E. Taylor, 1998: Data quality assessment methods for the Eastern Range 915-MHz wind profiler network. NASA Kennedy Space Center Contractor Rep. CR-1998-207906, 49 pp. [Available from ENSCO, Inc., 1980 N. Atlantic Ave., Suite 230, Cocoa Beach, FL 32931.]

——, F. J. Merceret, G. E. Taylor, and J. G. Ward, 2003: Performance of five 915-MHz wind profilers and an associated automated quality control algorithm in an operational environment. *J. Atmos. Oceanic Technol.,* **20,** 1488–1495.

Mak, M. K., and J. E. Walsh, 1976: On the relative intensities of sea and land breezes. *J. Atmos. Sci.,* **33,** 242–251.

Ohara, T., I. Uno, and S. Wakamatsu, 1989: Observed structure of a land breeze head in the Tokyo metropolitan area. *J. Appl. Meteor.,* **28,** 693–704.

Sen Gupta, P. K., and K. C. Chakravortty, 1947: Land breeze at Calcutta (Alipore). *Sci. Notes Meteor. Dept. India,* **9,** 73–80.

Simpson, J. E., 1996: Diurnal changes in sea-breeze direction. *J. Appl. Meteor.,* **35,** 1166–1169.

Stephan, K., C. M. Ewenz, and J. M. Hacker, 1999: Sea-breeze front variations in space and time. *Meteor. Atmos. Phys.,* **70,** 81–95.

Taylor, G. E., M. K. Atchison, and C. R. Parks, 1990: The Kennedy Space Center Atmospheric Boundary Layer Experiment. ENSCO Rep. ARS-90-120, 229 pp. [Available from ENSCO, Inc., 1980 N. Atlantic Ave., Suite 230, Cocoa Beach, FL 32931.]

Wakimoto, R. M., and N. T. Atkins, 1994: Observations of the sea-breeze front during CaPE. Part I: Single Doppler, satellite, and cloud photogrammetry analysis. *Mon. Wea. Rev.,* **122,** 1092–1114.

Wilson, J. W., and D. L. Megenhardt, 1997: Thunderstorm initiation, organization, and lifetime associated with Florida boundary convergence lines. *Mon. Wea. Rev.,* **125,** 1507–1525.

Yan, H., and R. A. Anthes, 1987: The effect of latitude on the sea breeze. *Mon. Wea. Rev.,* **115,** 936–956.

Zhong, S., and E. S. Takle, 1992: An observational study of sea- and land-breeze circulation in an area of complex coastal heating. *J. Appl. Meteor.,* **31,** 1426–1438.

——, and ——, 1993: The effects of large-scale winds on the sea–land-breeze circulations in an area of complex coastal heating. *J. Appl. Meteor.,* **32,** 1181–1195.